Stationary and Nonstationary Correlation-Frequency Analysis of Heterodyne Mode Laser Light Scattering: Magnitude and Periodicity of Canine Tracheal Ciliary Beat Frequency in Vivo

Tarun Chandra,*‡ Donovan B. Yeates,*§ Irving F. Miller,*‡ and Lid B. Wong*

Departments of *Medicine and ‡Chemical Engineering, University of Illinois at Chicago, and the §Veterans Administration West Side Medical Center, Chicago, Illinois 60612 USA

ABSTRACT Stationary and nonstationary correlation-frequency analysis of heterodyne laser light scattering were utilized to make automated, on-line, objective measurements of tracheal ciliary beat frequency (CBF) in intact, anesthetized canines. The stationary correlation-frequency analysis laser light-scattering technique was used to assess the magnitude of the CBF stimulatory responses induced by aerosolized 10^{-5} M fenoterol (sympathomimetic), and 10^{-8} M and 10^{-6} M methacholine (parasympathomimetic) delivered to the whole lungs of eight barbiturate-anesthetized beagles. The nonstationary correlation-frequency analysis laser light-scattering technique was used to measure the effect on tracheal CBF of increasing the cytosolic calcium ion concentration with a calcium ionophore, A23187. Aerosolized A23187 was delivered to the isolated tracheal lumens of eight beagle dogs in cumulative doses ranging from 10^{-9} M to 10^{-6} M. Administration of the ionophore synchronized the CBF with a period of 5.3 min. Dose dependencies were observed in both the time to the peak CBF stimulation and the magnitude of the stimulatory response. The magnitude of CBF stimulation was inhibited by prior administration of aerosolized nifedipine (2 mg/ml), a voltage-operated calcium channel blocker. The A23187-induced modulation period of tracheal CBF, was unchanged by nifedipine. These are the first data to demonstrate that the magnitude and periodicity of CBF are two independent coupled processes. The cooperativity of these two processes could be determinant in the effectiveness of mucociliary transport.

INTRODUCTION

In the mammalian respiratory tract, the effectiveness of mucus transport is governed by the ensemble metachronal behavior of the cilia. Ciliary activity can be characterized by their beat frequency and phase relationship as well as their temporal and spatial variation (Wong et al., 1993). Studies of ciliary beat frequency in vivo indicate that their responses to stimulating agents can be episodic or oscillatory in nature (Hameister et al., 1991; Harrison et al., 1992; Wong et al., 1990b). On inspection, such oscillations also appear to be embedded within the basal ciliary beat frequency (CBF). This raises the possibility that cilia may be regulated by independent mechanisms controlling the magnitude and periodicity of their beat frequency, representing further examples of common regulatory mechanisms for vital cellular functions (Rapp, 1987). The determination of such physiological regulatory mechanisms and responses of CBF is a fundamental step toward the ultimate goal of discovering how these phenomena relate to effective mucociliary transport.

The above-referenced initial observations indicating the time-variant nature of CBF and its response to stimulants were limited by the inability of the system to resolve details regarding their temporal characteristics (Hameister et al., 1991; Harrison et al., 1992; Wong et al., 1988a; 1990a, b; 1991; 1993). The correlation analysis heterodyne mode laser light-scattering system used to perform these early studies incorporated a 4-bit hard-wired correlator that limited both the adaptability of the signal processing and the throughput of the CBF measurements. The 20-s signal collection and analysis time together with the time alloted for data evaluation and storage limited the practical temporal resolution to one CBF measurement every 1 to 2 min. This 20-s signal collection time represents the minimum time to construct an autocorrelation function with the minimum number of channels, i.e., 80 channels, such that its inversion by fast Fourier transform (FFT) was indicative of a reliable CBF measurement.

The primary objectives of the research described herein were to increase the temporal resolution of the CBF measurements by incorporating software algorithms into the correlation analysis laser light-scattering (CALLS) system that would be more indicative of the magnitude and oscillatory nature of the ciliary beat and provide a more objective measurement system. We then used this system to better delineate and predictably manipulate the episodic nature of CBF.

To achieve these objectives, the heterodyne signal-to-noise ratio of the laser light-scattering system was maximized by increasing the bandwidth of the photon counter and the intensity of the laser. To measure the magnitude of the ciliary beat signal, the CALLS system was adapted further by incorporating a stationary signal autocorrelation-frequency analysis to process photon counting and calculate and display the CBF sequentially at 3-s intervals on a PC computer, independent of operator interaction. This system was evaluated with the same agents and animal model used to test the previous hard-wired correlator

Received for publication 30 July 1993 and in final form 30 December 1993.

Address reprint requests to Lid B. Wong, Ph.D., Section of Environmental and Occupational Medicine (M/C 788), Department of Medicine, University of Illinois at Chicago, 1940 W. Taylor St., Chicago, IL 60612.

0006-3495/94/03/878/13 $2.00

CALLS system (Wong et al., 1988a). To reveal the inherent periodic modulation of CBF in vivo, a nonstationary time-frequency analysis algorithm was implemented by combining adaptive signal processing, digital filtering, and nonstationary bilinear time-frequency transformation to perform noninterruptive near-real-time calculations of CBF. The power of this latter algorithm was demonstrated by showing that, in the trachea of the sedated dog in which the ganglionic nicotinic and cyclooxygenase pathways were inhibited, a calcium ionophore (A23187) caused a synchronous periodic modulation of CBF in which the magnitude regulatory mechanism was dependent on the membrane voltage-operated calcium channels, but in which the oscillatory response was not.

STATIONARY AND NONSTATIONARY CORRELATION-FREQUENCY ANALYSIS

Heterodyne mode laser light scattering

Heterodyne mode laser light-scattering system

The heterodyne mode CALLS system (Wong et al., 1988a), discussed in detail elsewhere, was modified to enable higher photon count rates and shorter data collection times. The modified system is schematically shown in Fig. 1. Briefly, a 0.79-mm beam from a nonattenuated 6-mW red He-Ne laser with a wavelength of 632.8 nm, operated in the fundamental TEM_{00} mode, was optically expanded 10-fold and divided into halves by a beam splitter. The transmitted portion of the beam was backscattered (scattering angle $\theta = 180°$) by a piece of Teflon which acted as a random depolarizing scatterer. The reflected half of the laser light was transmitted through a 30-cm-long, 8-mm outside diameter, 4.5-mm inside diameter stainless steel endotracheal probe. This beam was focused to a 7-μm spot size, 5 mm from the probe surface, using a 22-mm focal length uniform lens and a 2-mm square prism. A 5-mm-diameter glass window was used to seal the optics inside the probe. Photons backscattered from the cilia and the epithelium within the focal region were collected and transmitted back via the same optical path. At the beam splitter, these photons and the coincident photons backscattered from the Teflon were combined to yield a heterodyne "light beating" signal (Cummins and Swinney, 1970) based on constructive and destructive interference. In this case, the Doppler shifted photons from the beating cilia were demodulated by those photons that comprised the local oscillator, i.e., the backscattered photons from the epithelium and Teflon, which had not undergone the same Doppler shift. This signal was then collimated using a 25.4-μm pinhole. Any remnant reflecting light was largely eliminated by a polarizing analyzer. A plano-converging lens focused the resulting photons onto a photon-counting photomultiplier tube (R649, Hamamatsu). The photocurrent pulses from the photomultiplier tube were converted to voltage pulses by a fast preamplifier (9301, EG&G Ortec) and converted into TTL pulses using a 100-MHz pulse amplifier-discriminator (modified 9302, EG&G). Its adjustable gain ($\times$20 to $\times$200) and discriminator level (50 mV to 1 V) enabled optimization of the signal-to-noise ratio. The resulting TTL pulses were routed to a dual-port interfaced, 16-bit, multichannel scaler photon counting board (ACE, EG&G Ortec, 2 μs data to memory loading time), occupying a 16-bit ISA slot in the PC computer. The pulses were binned sequentially according to the chosen sampling time and the designated number of channels. To determine the underlying characteristics of the ciliary beat frequency, the temporal nature of each of the resulting sequences was analyzed using either stationary or nonstationary time-frequency distribution algorithms. The

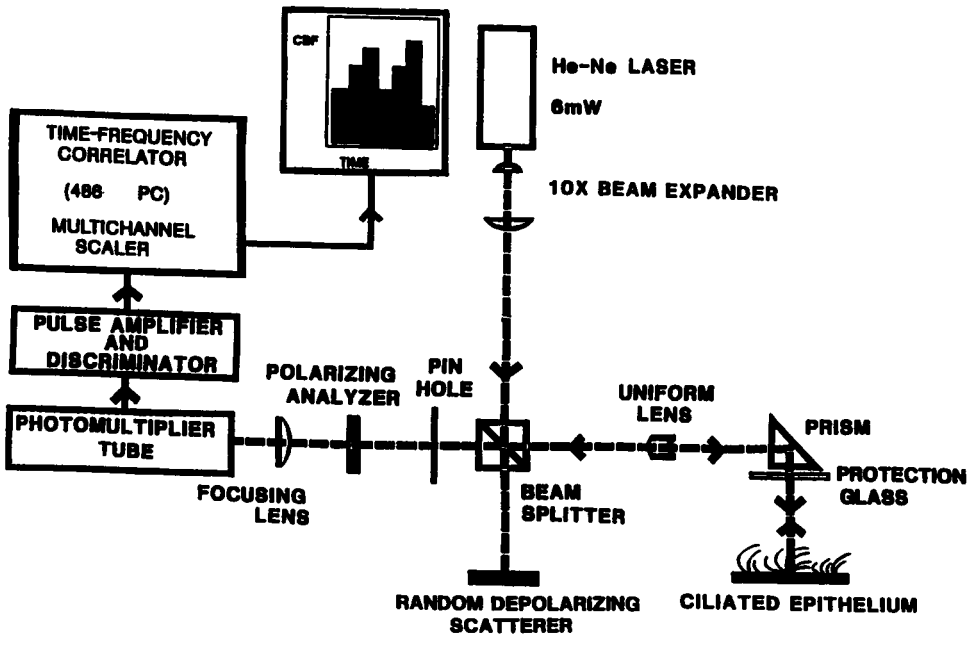

FIGURE 1 Correlation-frequency analysis heterodyne mode laser light-scattering system.

CBF values were displayed concurrently on a color monitor. This display was continuously updated to reflect the 100 most recent CBF values, enabling the experimenter to monitor an ongoing study. A 486-25 MHz PC computer (Northgate) yielded CBF values every 2.6 s and 4.8 s using the stationary and nonstationary algorithms, respectively. Both algorithms were developed using interactive C language (Microsoft C 5.1).

Stationary correlation-frequency analysis of heterodyne laser light scattering

Heterodyne mode correlation analysis of laser light scattering is utilized for detecting non-Gaussian light scattering fields (Jakeman, 1974), as opposed to the Siegert relation between the normalized, single-clipped intensity autocorrelation function, $g^{(2)}(\tau)$, and the electric field autocorrelation function, $g^{(1)}(\tau)$ (Jakeman, 1974; Loudon, 1983).

$$g^{(2)}(\tau) = 1 + \mathscr{S}|\, g^{(1)}(\tau)\,|^{(2)} \tag{1}$$

The equivalent expression for heterodyne scattering is,

$$g^{(2)}_{\mathrm{HET}}(\tau) = 1 + \frac{2\bar{n}_s\bar{n}_o}{(\bar{n}_s + \bar{n}_o)^2}\,\mathrm{Re}(g^1(\tau))\cos(\tau\Delta\omega) + \frac{\bar{n}_s^2}{(\bar{n}_s + \bar{n}_o)^2}|\, g(\tau) - 1\,|^2 \tag{2}$$

where $\mathscr{S}$ and Re are the complex and real notations, respectively, n_s and n_0 are the mean photon count rates of the scattered and reference beams (local oscillator), respectively, and $\Delta\omega$ is the difference between the Doppler shifted photons and the scattered photons from the local oscillator. The second term on the right in Eq. 2 represents the heterodyne component, and the third term represents the homodyne intensity fluctuation component of the autocorrelation function. By inspection, the heterodyne component can be made to dominate over the homodyne component by increasing the ratio of n_0 to n_s. For a Lorentzian source (laser), the heterodyne component of the autocorrelation function is an exponentially decaying cosine function representing the CBF periodicity embedded in $g^{(2)}_{\mathrm{HET}}(\tau)$ (Wong et al., 1988a; Lee and Verdugo, 1976). After the Wiener-Khintchine theorem, the periodicities of $g^{(2)}_{\mathrm{HET}}(\tau)$ can be represented as the predominant peak of the power spectrum.

To determine the CBF from the periodicity of the heterodyne signal from the ciliated epithelium as detected by the CALLS system, judicious choices of sampling time, photon sequences, collection time, and digital signal analysis need to be incorporated into the algorithm to calculate $g^{(2)}_{\mathrm{HET}}(\tau)$. By maintaining a 0.1% allowable statistical error in the normalized autocorrelation function as in the CALLS system, i.e.,

$$\frac{\Delta g^{(2)}_{\mathrm{HET}}}{g^{(2)}_{\mathrm{HET}}} = 0.001 \tag{3}$$

assuming a ratio (α) of 0.01 between the coherent and incoherent part of the optical signal, and increasing the average number of photon counts per channel per sample time ($\langle n \rangle$) to 5000, the minimum number of iterative calculation cycles, C, that have to be added to yield a true estimate of the normalized intensity autocorrelation function, $g^{(2)}_{\mathrm{HET}}$, is given by (Wijnaendts van Resandts, 1974).

$$C = \left\{ \frac{g^{(2)}_{\mathrm{HET}} 1}{\Delta g^{(2)}_{\mathrm{HET}}} \frac{1}{\alpha \langle n \rangle} \right\}^2 = 400 \tag{4}$$

This was achieved by obtaining a 256-point autocorrelation function from a 756-channel continuous photon count sequence. This sequence was obtained by binning the TTL pulses sequentially in 756 channels, each of 3-ms duration (see below for the choice of sampling time). This results in 500 sequential iterative calculations. To enhance the signal-to-noise ratio resulting from the calculation of the autocorrelation function, single bit quantization (also known as single-clipped photon counting (Jakeman, 1974)) was implemented in the software to process the TTL pulse sequences from the photon counting system.

The clipped count, n_k, is defined as,

$$n_k(t) = \begin{cases} 1, & n(t, T) > k \\ 0, & n(t, T) \le k \end{cases} \tag{5}$$

where k, is the clipping level and $n(t, T)$ is the unclipped count rate at time t for a sampling T. The ith channel of the unnormalized intensity autocorrelation function of 256 channels was calculated by shifting the sequence one channel at a time,

$$g^{(2)}_{\mathrm{HET}}(iT) = \sum_{j=257}^{756} n(j) n_k(j - i) \tag{6}$$

where $i = 1256 \wedge T = 3$ ms/channel. The mean of the photon counts, $\bar{n}$, was used to normalize the autocorrelation function (Oliver, 1974; Oliver, 1980). The normalized autocorrelation function, $g^{(2)}_{\mathrm{HET}}(\tau)$, was then calculated as,

$$g^{(2)}_{\mathrm{HET}}(iT) = \sum_{j=257}^{756} \frac{n(j) n_k(j - i)}{\sum_{l=j-256}^{j=1} n(l) \sum_{l=j-256}^{j=1} n_k(l)} \tag{7}$$

The slopes of the autocorrelation functions were estimated by linear regression and those which were not consistent with an exponential decaying function were discarded. To obtain approximately 1 Hz frequency resolution, the remaining autocorrelation functions were inverted by a 256-point fast Fourier transform (FFT) algorithm. Using a short data batch algorithm (Oliver, 1979), the absolute values of the real parts of the amplitudes were used for estimating the power spectra, as given by the equation

$$S(\omega) = \mathrm{Re} \sum_{j=0}^{255} g^{(2)}_{\mathrm{HET}}(jT)\, e^{-i\omega jT} \tag{8}$$

where $i = \sqrt{-1}$. The dominant peak in each power spectrum was defined as the CBF.

By increasing the bandwidth of the photon counting board and the intensity of the laser in the new system, the increase in photon counts per channel $\langle n \rangle$ enabled reduction of the

data collection time per CBF measurements from 20 s to 2.27 s as compared with the hard-wired correlator CALLS system. This resulted in each CBF measurement time being reduced from 1 to 2 min to 2.6 s without loss in accuracy.

Nonstationary correlation-frequency analysis of heterodyne mode of laser light scattering

Investigations into the nature of ciliary activity indicate that the cilia beat in a coordinated manner within the envelope of the traveling metachronal wave. Both the CBF and the metachronal wave have been shown to be time variant (Wong et al., 1993). In the previous section, as in most initial approximations of biological phenomena that exhibit periodic behavior, we have used stationary signal analysis to derive the magnitude of the tracheal CBF. We now apply recent developments in nonstationary signal analysis (Cohen, 1989; Hlawatsch and Boudreaux-Bartels, 1992) to more closely represent the underlying oscillatory biological phenomena and thus reveal new insights into the nature and regulation of CBF.

The utilization of nonstationary analysis to determine the time dependence of CBF is based on the presumption that information intrinsic to the time-variant behavior of the cilia is embedded within the photon TTL sequences derived from the heterodyne signal. In general, a time-varying, nonstationary signal can be represented by the Cohen class of time-frequency distribution (Cohen, 1966; 1989)

$$C(t, \omega, \phi) = \frac{1}{2\pi} \int\int\int e^{j(u\theta - \tau\omega - \theta t)} \phi(\theta, \tau) \cdot f\left(u + \frac{\tau}{2}\right) f^*\left(u - \frac{\tau}{2}\right) du\, d\tau\, d\theta \quad (9)$$

where $f(t)$ is the time-varying signal, $\phi(\theta, \tau)$ is the kernel function and ω is the frequency; * indicates complex conjugation, $f(u+\tau/2)f^*(u - \tau/2)$ is the local autocorrelation and $e^{i(u\theta - \tau\omega - \theta t)}$ is the Fourier transform integrand. The kernel in Eq. 9 is not a function of time or frequency and is independent of the signal. As the signal is iterated twice within the transform, the resultant distribution is bilinear. This also assures that the distribution is time and shift invariant (Cohen, 1989).

The implementation of this equation to derive the time-frequency distribution results in the calculation of both auto (signal) and cross (interference) terms. The suppression of the cross terms and the enhancement of the auto terms can be optimized using a kernel, $\phi(\theta, \tau)$ which is not a function of time and frequency and is independent of the signal. Thus, the continuous, real, bilinear time-frequency distribution is,

$$E(t, \omega) = \int_{-\infty}^{\infty} e^{-j\omega\tau} \left[\int_{-\infty}^{\infty}\int_{-\infty}^{\infty} e^{j(\theta u - \theta t)} \phi(\theta, \tau) \cdot f\left(u + \frac{\tau}{2}\right) f^*\left(u - \frac{\tau}{2}\right) d\theta\, du \right] d\tau \quad (10)$$

and its corresponding discrete form is,

$$E_D(n, k) = 2 \sum_{\tau=-\infty}^{\infty} W_N(\tau) e^{-(j2\pi k\tau/N)} \cdot \left[\sum_{u=-\infty}^{\infty} \int_{-\infty}^{\infty} d\theta e^{j(\theta u - \theta t)} \phi(\theta, \tau) f(n + u + \tau) f^*(n + u - \tau) \right] \quad (11)$$

where n and k are the time index and frequency index, respectively.

To implement the discrete form of Eq. 11, we utilized noise reduction techniques. A single bit quantization was used to convert the photon sequences into binary sequences. To avoid aliasing effects caused by a periodicity of π in $E(t, \omega)$, the real-valued time signal, $f_r(t)$, was converted into its complex-valued form, $f(t)$, using the Hilbert transform (Choi and Williams, 1989; Oppenheim and Schafer, 1975). The resultant transformed signals were subjected to a double-clipping, local autocorrelation. This autocorrelation was then convolved with a moving rectangular window exponential kernel known as the Choi-Williams kernel (Choi and Williams, 1989). The time-frequency spectrogram was derived by applying the Cooley-Tukey discrete Fourier transform. The CBF was defined as the predominant peak of each spectrogram.

SIGNAL ENHANCEMENT AND NOISE REDUCTION

Single bit quantization was applied to the TTL sequences using Eq. 5 described above.

An analytical signal of a causal sequence in terms of the Hilbert transform is the odd and even sequences of the real and imaginary parts of the FFT or, simply the Z-transform within the region of convergence (Oppenheim and Schafer, 1975). Thus, to obtain the analytical signal from the real-valued photon count sequence (512 channels long; see below for channel numbers selection) using the Hilbert transformation (Choi and Williams, 1989), the clipped photon counts ($k = n$) were fast Fourier transformed using the Cooley-Tukey algorithm. The magnitudes of the positive frequency terms and negative frequency terms were multiplied by 2 and 0, respectively, whereas the DC term (zero frequency) was left unchanged. The inverse FFT of this sequence yielded the real and imaginary components of the analytical signal.

Double-clipped local autocorrelation analysis, a technique for detecting weak signals in the presence of strong noise for photon-scattering signals (Oliver, 1980), was applied to the CBF Doppler signal.

$$g_k^{(2)}(\tau) = \langle n_k(t) n_k(t + \tau) \rangle \quad (12)$$

where $\langle\ \rangle$ denotes ensemble averaging. By implementing the clipping level as the average photon count rate of the sample, Eq. 12 adequately represents the spectral characteristics of the unclipped photon sequence (Oliver, 1974). This also ensures that the maximum contribution of noise

to the autocorrelation function is one count/channel (Oliver, 1974).

For multicomponent signals, the exponential kernel (Choi and Williams, 1989),

$$\phi(\theta, \tau) = e^{-(\theta^2\tau^2/\sigma)} \tag{13}$$

has a distinct advantage over other kernels. It preserves the signal energy marginals and suppresses undesirable cross-terms in the frequency spectrum caused by interference between the individual frequency components, with little autocomponent broadening. Using this kernel in Eq. 11 yields the discrete form of the Choi-Williams time-frequency distribution,

$$E_D(n, k) = 2 \sum_{\tau=-\infty}^{\infty} W_N(\tau) e^{-(j2\pi k\tau/N)} \cdot \left[\sum_{u-\infty}^{\infty} W_M(u) \frac{e^{-(u^2/[4\tau^2/\sigma])}}{\sqrt{4\pi\tau^2/\sigma}} f(n+u+\tau) f^*(n+u-\tau) \right] \tag{14}$$

where W_N and W_M are symmetrical weighting windows. The choice of the scaling factor, σ, determines the compromise between the enhancement of the auto-terms and suppression of the cross-terms. Large values of σ (>1) are used for rapidly changing signals, and small values ($\leq$1) are used for gradually changing signals (Choi and Williams, 1989). This was tested by applying Eq. 14 to analyze a simulated chirp signal consisting of dual frequencies varied with respect to time.

IMPLEMENTATION AND OPTIMIZATION OF THE NONSTATIONARY ALGORITHM

Choi-Williams distribution for measuring tracheal CBF

To estimate CBF, the discrete form of the Choi-Williams distribution, Eq. 14, was implemented with the rectangular windows, W_N and W_M of unit magnitude and of lengths 256 and 129, respectively. The distribution was calculated only for the middle (256th) channel of the photon count sequence. The scaling factor, σ, was initialized to one but was recalculated for subsequent CBF samples as the ratio of the previous two CBF values. In this way σ adapted to temporal changes in CBF. The analytical form of the photon count sequence was used as the time-varying signal. To prevent 60 Hz electrical or optical interference from affecting the CBF measurements, frequencies <50 Hz were used for selecting the predominant peak from the frequency spectrum. The occurrence of CBF values >50 Hz, as determined from previous studies, is minimal (Hameister et al., 1991; Harrison et al., 1992; Wong et al., 1988a; 1990a, b; 1991; 1993).

Linewidth error

Reliable estimation of the CBF from the heterodyne signal requires minimization of the linewidth error for such a Gaussian-Lorentzian laser light-scattering system. The percentage error in linewidth, Γ, is measured as (Jakeman, 1974; Oliver, 1980),

$$\frac{\delta\Gamma}{\Gamma} = \frac{1.4T}{\bar{n}_s}\sqrt{\frac{\Gamma}{\Xi}} \tag{15}$$

where Ξ is the total duration of the signal, n_s, is the mean signal count rate per channel, and T is the sample time per channel. For a decrease in the total duration for photon sequences collection time per CBF measurement from 20 s (typical for the hard-wired Langley-Ford correlator CBF measurements (Hameister et al., 1991; Harrison et al., 1992; Wong et al., 1988a; 1990a, b; 1991; 1993), to 1.5 s (for the current system using the PC computer), the required percentage increase in signal photon count rate to maintain the same linewidth error, with other conditions remaining constant, is 365. These conditions were met by utilizing an unattenuated He-Ne laser power greater than 6 mW and together with a faster photon-counting system.

Choice of sampling time (T)

The reliability of correlation-frequency analysis of a signal embedded in a noisy environment is a function of sampling time and the total duration of data collection. Singular value decomposition analysis (Golub and Van Loan, 1983; Haykin, 1991) is a documented technique for analyzing noisy autocorrelation functions obtained from laser light-scattering experiments on polydisperse mixtures to yield particle size information (Finsy et al., 1989). To determine the optimal sampling time of our laser system, singular value decomposition was applied to the stationary autocorrelation functions obtained from stroboscopic light signals.

For a laser light-scattering system operated in the ambient environment, dust is the predominant contributor to noise. The normalized, single-clipped autocorrelation function of the heterodyne mode correlation analysis of laser light scattering, in the presence of spurious dust scattering, can be written as,

$$\begin{aligned} g^{(2)}_{\mathrm{HET}}(\tau) = 1 &+ \frac{2\bar{n}_o\bar{n}_s}{\bar{n}_t^2} q_s^{(1)}(\tau)\cos(\omega_s\tau) \\ &+ \frac{2\bar{n}_o\bar{n}_d}{\bar{n}_t^2} g_d^{(1)}(\tau)\cos(\omega_d\tau) \\ &+ \frac{\bar{n}_s^2}{\bar{n}_t^2} |\, g_s^{(1)}(\tau)\,|^2 \\ &+ \frac{\bar{n}_d^2}{\bar{n}_t^2} |\, g_d^{(1)}(\tau)\,|^2 \end{aligned} \tag{16}$$

where ω_s and ω_d are the Doppler shift frequencies of the signal and dust, respectively, and $\bar{n}_t = (\bar{n}_o + \bar{n}_s + \bar{n}_d)$. If the signal is strong enough such that $\bar{n}_s > \bar{n}_d$ the last term in Eq. 16 can be attributed to noise and discarded. Expressing the cosine functions as complex exponentials,

$$\cos(\omega\tau) = \frac{e^{(i\omega\tau)} + e^{(-i\omega\tau)}}{2} \tag{17}$$

and the field autocorrelation function as,

$$g_s^{(1)}(\tau) = e^{(-\Gamma_s \tau)} \tag{18}$$

$$g_d^{(1)}(\tau) = e^{(-\Gamma_d \tau)} \tag{19}$$

where Γ_s and Γ_d are the decay rates, the autocorrelation function can be rewritten as,

$$g_{\text{HET}}^{(2)}(jT) = 1 + \frac{\bar{n}_\sigma \bar{n}_s}{\bar{n}_t^2}(e^{-\lambda_1 jT} + e^{-\lambda_2 jT}) + \frac{\bar{n}_\sigma \bar{n}_d}{\bar{n}_t^2}(e^{-\lambda_3 jT} + e^{\lambda_4 jT}) + \frac{\bar{n}_s^2}{\bar{n}_t^2} e^{-\lambda_5 jT} \tag{20}$$

where $\lambda_2 = \lambda_1^*$; $\lambda_4 = \lambda_3^*$. Thus,

$$g_{\text{HET}}^{(1)}(jT) = \sum_{k=1}^{n} \alpha_k \beta_k^j \tag{21}$$

where $\beta_k = e^{-\lambda_k \tau}$

To estimate the multiple exponential decay rates, the Ziegler and McEwen algorithm was used (Zeiger and McEwen, 1974). Using

$$g_{\text{HET}}^2(jT)|_{j=1,2,\ldots,2m} \tag{22}$$

the $(m \times m)$ Hankel matrices H and H^s are constructed from the noisy autocorrelation function

$$H_{xy} = g_{\text{HET}}^{(2)}((x + y -)T) \qquad H_{xy}^3 = g_{\text{HET}}^{(2)}((x + y)T) \tag{23}$$

$$x, y = 1, 2, \ldots, m$$

To determine the effective rank of H (the data matrix presumably consisted of only the signal), singular value decompositions of H were performed,

$$H = USV^T \tag{24}$$

where U and V^T are orthonormal matrices such that $U^T \cdot U = V \cdot V_T = I$, S is a diagonal, nonnegative matrix containing the singular values of H in descending order of magnitude, i.e., $S(i, i) \geq S(i + 1, i + 1) \geq 0$.

If there is an abrupt decrease in the singular values, i.e., there exists an index j such that,

$$S(1, 1) \approx S(2, 2) \approx S(j, j)$$

$$\gg S(j + 1, j + 1) \geq \cdots \geq S(m, m) \geq 0 \tag{25}$$

then all singular values with magnitude less than $S(j, j)$ are due to noise and can be set to zero. j is then the effective rank of H.

To obtain the exponential factors, β_k, the submatrices U_j and V_j, consisting of the first j columns of U and V, respectively, and the $j \times j$ matrix S_j, were constructed. The matrix, W, was obtained from,

$$W = S_j^{-(1/2)} U_j^T H^s V_j S_j^{(1/2)} \tag{26}$$

The diagonal eigen-matrix, E, of W was obtained from,

$$W = XEX^{-1} \tag{27}$$

The eigenvalues of E, e_k $(k = 1, \ldots, n)$, are the exponential factors. The coefficients, α_k, were obtained from least-square analysis on Eq. 21 using the exponential factors, β_k.

To select the optimal sampling time for our nonstationary correlator, the following procedure was utilized. The behavior of the "Gaussian" CBF signal (Wong et al., 1988a) was approximated by an adjustable duty cycle and continuously variable intensity signal. Using a 10-Hz, stroboscopic light source (model 964A, Ametek), 10 samples of normalized, heterodyne, single-clipped autocorrelation functions (256 channels) were obtained from a 2048-channel-long photon count sequence. This light source was diffusely focused and placed directly in the optical path of the laser beam in front of the CBF probe. The signal was sampled using a sampling time, T, of 0.5 ms. The process was repeated for $T = 1$, 2, 3, 4, and 5 ms. The autocorrelation function decomposition, using the algorithm discussed above, was performed on an IBM-3090 mainframe computer using IMSL subroutines. The rank of the Hankel matrix, H, could not be determined by inspection. This indicated the autocorrelation functions were very noisy. Hence, the rank of H was cut off at 2, 3, 4 . . . 9 singular values (Finsy et al., 1989; Haykin, 1991), the corresponding exponential factors determined and an estimate for the strobe frequency obtained for each of the 10 samples for each sampling time. Root mean square deviations (RMSD) of the strobe frequency estimates were obtained from,

$$\text{RMSD} = \sqrt{\sum_{l=1}^{10} \left(\frac{\omega_1}{10} - 1\right)^2} \tag{28}$$

for each sampling time, using each singular value cutoff from 2 to 9, as shown in Fig. 2. As is evident, the 2-, 3-, and 4-ms sampling times yield their respective RMSD minima at the 6th singular value cutoff, which is the theoretically determined number from Eq. 19. To achieve the goal of a frequency resolution less than 0.5 Hz with a minimum data acquisition time, the 3-ms sampling time was optimal.

When the same procedure was used to analyze autocorrelation functions in the absence of a strobe light, all the

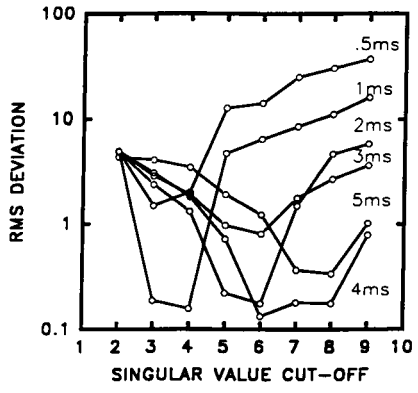

FIGURE 2 Root mean square autocorrelation values of 10-Hz strobe signal sampled at each designated sampling time resulting from singular value decomposition analysis.

sampling times yielded minima in their RMSD vs SV cut-off graphs (Fig. 3) at four singular values. The theoretical estimate for the number of singular values obtained from Eq. 19 is also 4.

Choice of total channel number (*N*)

For a 3-ms sampling time, the minimum number of channels, *N* (power of 2), which could provide a frequency resolution of approximately 1 Hz, was found to be 256. Thus, by taking into account of the analytic conversion of the photon sequences by the Hilbert transform, 512 channels of the data corresponding to 1.536 s of data collection time, were required for every CBF calculation.

TESTING THE NONSTATIONARY ALGORITHM FOR MEASURING CBF

The system was evaluated by two methods. First, the systems' dynamic range and accuracy between 2 and 50 Hz were evaluated using stroboscopic light. Second, the system's capabilities in distinguishing white noise spectra resulting from epithelium without ciliary motion and "light beating" Doppler spectra resulting from epithelium with undulating ciliary activity were evaluated. This was achieved by comparing the measurements obtained in vivo from electrocautry-burned epithelium covered with collagen-fibroblast matrix with those obtained from healthy ciliated epithelium from the same animal.

The stroboscopic light source (model 964A operated at 50% duty cycle, Ametek) was placed directly in the optical path of the laser beam emerging from the window of the CBF probe. Using a 3-ms sampling time the system was calibrated using the stroboscope over a 2- to 50-Hz frequency range. A linear correlation coefficient of $R^2 = 0.9997$ between the frequencies of the stroboscopic light and those measured by the system was obtained (Fig. 4).

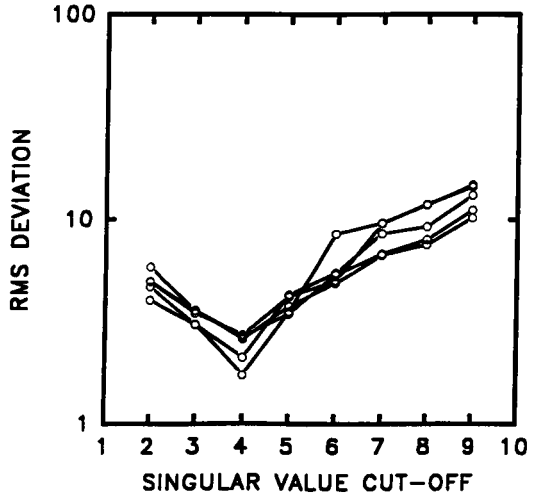

FIGURE 3 Background sampled at 0.5, 1, 2, 3 and 5 ms/channel yielded minima RMS deviation at fourth singular values.

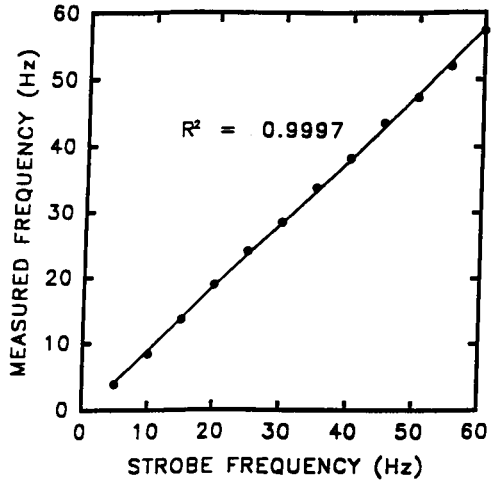

FIGURE 4 Comparisons of the strobe frequency to the frequency obtained by the nonstationary correlation-frequency analysis of heterodyne laser light-scattering system.

To create an area of tracheal epithelium without ciliary activity, the anterior tracheal wall was opened in one beagle and a 1-cm circumferential defect was created on the ciliated epithelium at the midlevel tracheal region using electrocautery techniques. The burned region was layered with autologous fibroblast-cartilage lattices (Duff et al., 1992). The dog was allowed to heal and returned later for measurements of tracheal CBF. The dog was anesthetized with pentobarbital using the experimental protocols described below, and CBF measured using the nonstationary algorithm. The focal spot of the laser light-scattering probe was guided to the fibroblast-cartilage region using a fiber-optic bronchoscope, where there was no ciliary activity. After the dog's physiological parameters were stabilized, measurements were made for approximately 30 min. The experiment was repeated by adjusting the probe outside of the matrix fibroblast-cartilage region where there was ciliary activity. Fig. 5, *a* and *b*, shows the time-frequency measurements obtained from the ciliated and nonciliated regions, respectively. The measurements obtained from the nonciliated region demonstrated a predominance of low-frequency noise measurements (<1 Hz) throughout the measuring period. The measurements obtained from the ciliated area showed a mean CBF of 6.2 ± 8.2 Hz.

MAGNITUDE AND PERIODICITY OF CANINE TRACHEAL CILIARY BEAT FREQUENCY IN VIVO

We evaluated the performance of the new innovations incorporated into the CALLS system. The stationary algorithm was tested by measuring the magnitude of the stimulatory responses in tracheal CBF induced by the two autonomic agonists, whose predictable responses were previously demonstrated using the hard-wired autocorrelator (Wong et al., 1988a). The nonstationary algorithm was used to measure the predictable rapid temporal stimulation of tracheal CBF due to an increase in intracellular calcium (Di Benedetto et al.,

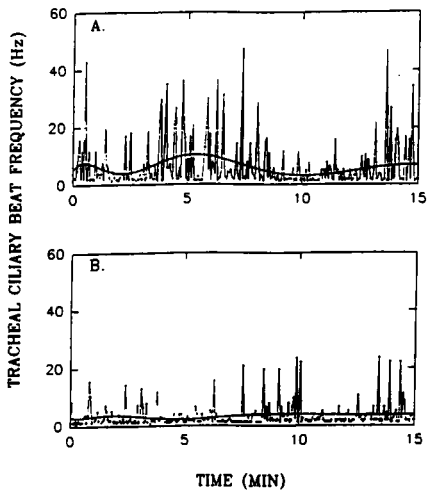

FIGURE 5 (*A*) Measurements of ciliary beat frequency from the ciliated area. Cyclical nature of CBF was highlighted by 10th order regression curve (solid line). (*B*) Measurements of ciliary beat frequency from the electroporated tracheal ciliated area cover with fibroblast-matrix.

1991; Dirksen and Sanderson, 1990; Girard and Kennedy, 1989; Villalon et al., 1989) and to investigate possible mechanisms that may have led to our observations.

Ciliary activity is regulated via autonomic pathways (Yeates et al., 1992). Tracheal CBF has been shown to be stimulated in vitro (Wong et al., 1988a) and in vivo (Wong et al., 1988b) by luminal application of the beta 2 adrenergic agonist, fenoterol, and the muscarinic cholinergic agonist, methacholine.

Increases in respiratory ciliary activity have been shown to be related to an increase in intracellular calcium caused by receptor-operated mechanisms and ionophores (Di Benedetto et al., 1991; Dirksen and Sanderson, 1990; Girard and Kennedy, 1989; Villalon et al., 1989). Cytosolic calcium concentrations have been shown to fluctuate in a periodic manner in several cell types. We questioned whether any observed periodicity of CBF or increase in its magnitude due to administration of the calcium ionophore, A23187 (a structure which increases transport of divalent Ca^{2+} into the cell across the plasma membrane (Pressman, 1976)), was mediated via voltage-operated calcium channels.

EXPERIMENTAL PROTOCOL

The experimental procedure and specific protocols were approved by the Committee on Animal Care of the Biological Resources Laboratory of the University of Illinois at Chicago, which is approved by the American Association for Accreditation of Laboratory Animal Care (AAALAC).

Animal preparation

Two studies, I and II, were performed using two cohorts, each comprising eight beagles. The animal preparation procedure has been described previously (Hameister et al., 1991; Harrison et al., 1992; Wong et al., 1988a; 1990a, b; 1991; 1993). In brief, each dog was fasted 12 h before each study, but allowed free access to water. The animal was sedated with acepromazine (0.55 mg/kg), delivered subcutaneously, and barbiturate-anesthetized with either 2.5% Surital, a short-acting barbiturate (study I), or 25 mg/kg pentobarbital, a long-acting barbiturate (study II), delivered intravenously through a 22-gauge in-dwelling catheter. The level of the anesthetic was maintained during the experiment by intermittent injections of barbiturates through the catheter. The dog was intubated with a size 6 endotracheal tube and placed in the supine position on an operating table. The upper jaw was secured to the table by a gauze strip. The body temperature was stabilized using external heating pads and water blankets. EKG, rectal temperature, and depth of anesthesia were monitored constantly throughout the experiment. A mechanical ventilator (Harvard) was used to maintain eucapnic conditions as indicated by CO_2 and O_2 monitors, which continuously sampled the inspired oxygen (F_{IO_2}) and expired carbon dioxide concentrations. A pulse oximeter (Datex) was attached to the tongue for continuous monitoring of oxyhemoglobin saturation. The light-transmitting endotracheal probe was guided into the trachea and positioned to allow the laser to illuminate the ventral surface of the ciliated epithelium. After a 15- to 20-min period, during which the laser photon counts and the physiological parameters were stabilized, 10 min of baseline tracheal CBF were acquired from each animal.

In study I, the stationary algorithm was tested using aerosolized parasympathomimetic and sympathomimetic agents delivered to the whole lungs of anesthetized beagles. The dog was intubated with its endotracheal (ET) tube cuff inflated near the larynx such that aerosols were delivered to the whole lungs including the trachea.

In one experiment, each animal was challenged once with the test agents, 10^{-8} M methacholine in 0.9% saline and 10^{-6} M methacholine in 0.9% saline aerosolized with an ultrasonic nebulizer (Devilbiss) and administered to the whole lung. The nebulizer was connected to the inspiratory line of the ventilation circuit. Postchallenge CBF_t was measured for 20 min for each test agent. In a second experiment, each animal was challenged with 10^{-6} M fenoterol in 0.9% saline in a similar fashion and CBF_t was acquired during the subsequent hour.

In study II, the nonstationary algorithm was tested using calcium ionophore A23187 delivered exclusively to the tracheal lumen of anesthetized beagles. Preliminary experiments were performed before the formal studies, to determine the doses of the calcium ionophore (A23187), the voltage-operated calcium channel blocker (nifedipine), and the time required for CBF to reach steady-state baseline values.

A size 6 ET tube was inserted distal to the larynx and ventral to the probe and its cuff inflated near the carina, thus isolating the tracheal lumen from the intrapulmonary airways. An additional size 4 ET tube for aerosol delivery exclusively to the tracheal lumen was inserted immediately distal to the larynx and ventral to the light transmitting ET

probe. Each dog was stabilized for a minimum of 30 min, during which time the temporal behavior of CBF was continuously monitored on the video monitor of the automated system. Baseline CBF measurements were obtained for 10 min. Hexamethonium bromide (4 mg/kg, dissolved in 0.9% saline), a ganglionic nicotinic blocker, and indomethacin (4 mg/kg, dissolved in 50 mEq $NaHCO_3$), a cyclooxygenase inhibitor, were administered intravenously. CBF was subsequently monitored for the next 20 min. Dimethyl sulfoxide (1:3 ratio diluted with 0.9% saline to 10 cc, Sigma), the solvent for A23187 and nifedipine, was aerosolized using an ultrasonic nebulizer (Devilbiss, operated at position 9) and delivered to the isolated tracheal lumen for 2 min via the inspiratory line of the ventilation circuit. CBF was monitored for the next 20 min. To increase the intracellular calcium level through nonreceptor mechanisms, 10^{-9}, 10^{-8}, 10^{-7}, and 10^{-6} M aerosolized A23187 (1.9×10^{-3} M stock was dissolved in dimethyl sulfoxide in 1:3 ratio, diluted with 0.9% saline and stored at 0°C) were delivered to the tracheal lumen. CBF was acquired for 20 min after each challenge. The calcium channel blocker, nifedipine (2 mg/ml), was then delivered in an identical fashion, followed by 20 min of CBF acquisition. The isolated tracheal lumen was then rechallenged with the same four doses of the ionophore, separated in time by 20 min during which tracheal CBF was monitored. At the end of each experiment, 10 min of postchallenge baseline was obtained.

All data are expressed as means ± SE unless otherwise specified. All statistics were analyzed by unbalanced, two-way analysis of variance using the raw CBF data.

RESULTS

Physiological parameters, such as percent oxygen saturation of arterial blood (Spo_2), expired carbon dioxide (Eco_2), electrocardiogram, and rectal temperature remained stable throughout the course of the experiments. From the end Eco_2 measurements, it was determined that eucapnic ventilation had been maintained throughout the experiments.

Study I. Stimulatory responses of tracheal CBF induced by fenoterol and methacholine

The mean baselines, averaged over a 10-min interval in eight beagle dogs, for the methacholine and the fenoterol studies were 6.5 ± 0.1 Hz (mean ± SE) and 5.6 ± 0.1 Hz, respectively. Two-minute aerosol exposures to 10^{-8} M methacholine, 10^{-6} M methacholine, and 10^{-6} M fenoterol stimulated tracheal CBF to mean maxima of 14.0 ± 0.7 Hz ($p < 0.05$), 15.8 ± 2.2 Hz ($p < 0.05$), and 15.4 ± 1.0 Hz ($p < 0.05$), respectively. These results are consistent with those obtained on the CALLS system using the 4-bit hard-wired correlator (1096, Langley-Ford correlator system Wong et al., 1988).

Study II. Temporal responses of tracheal CBF induced by calcium ionophore

Baseline CBF exhibited intrinsic periodicity. When a 1-min (13 data point) moving average (1MMA) was performed on the mean CBF data of all eight dogs, the baseline CBF was observed ranging between 7 and 10 Hz. The 1MMA serves as a high-frequency noise filter. The CBF was synchronized by the ionophore challenge, as indicated by the oscillatory nature of Fig. 6. Power spectrum analysis of the 10^{-6} M ionophore response revealed a predominant period of 5.3 min. The periodicity of the CBF response to the ionophore was not affected by the pretreatment with aerosolized nifedipine, because the power spectrum of the 10^{-6} M ionophore challenge response yielded the same dominant period as the pre-nifedipine challenge of the same A23187 dose.

When the area under the CBF-time plot (Fig. 6), averaged across all eight dogs, was plotted as a function of the ionophore dose, it was evident that aerosolized A23187 challenge stimulated tracheal CBF in a dose-dependent manner, as shown in Fig. 7. At ionophore doses of 10^{-7} M and 10^{-8} M, the values were significantly greater than baseline ($p < 0.001$). The mean maximal stimulation of tracheal CBF, obtained from the 1MMA procedure, was 11.6 ± 0.9 Hz and 13.2 ± 1.4 Hz, respectively, for the two doses. The aerosolized nifedipine challenge (2 mg/ml) attenuated the magnitude of the stimulation of tracheal CBF when the dogs were

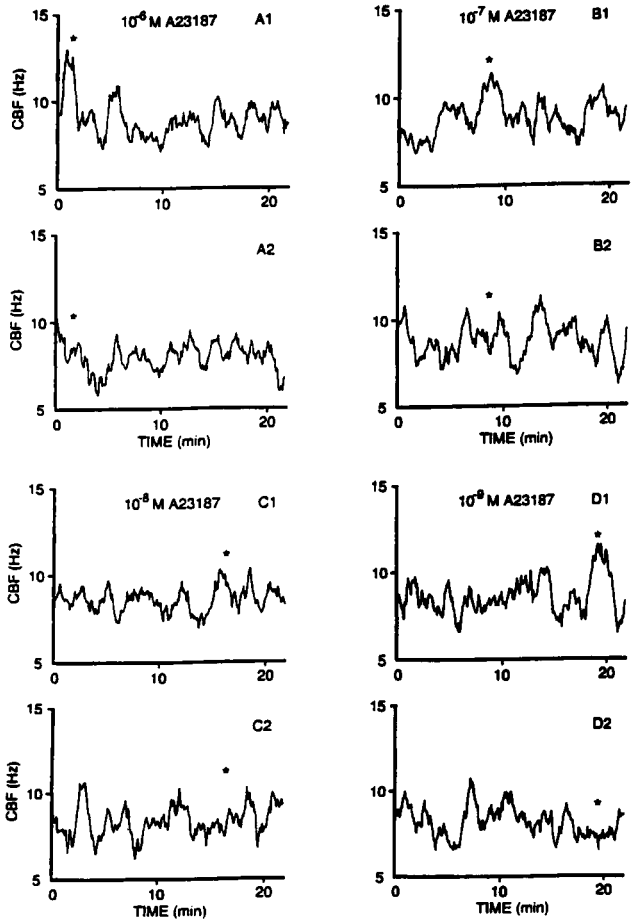

FIGURE 6 Effect of 10^{-6} M, 10^{-7} M, 10^{-8} M, and 10^{-9} M A23187 challenge on tracheal CBF (average of eight dogs) (*A1, B1, C1, D1*) without and (*A2, B2, C2, D2*) with prior treatment of nifedipine. Aerosolized A23187 was delivered at time zero. * represents the predominant magnitude stimulatory responses induced by A23187 without and with nifedipine.

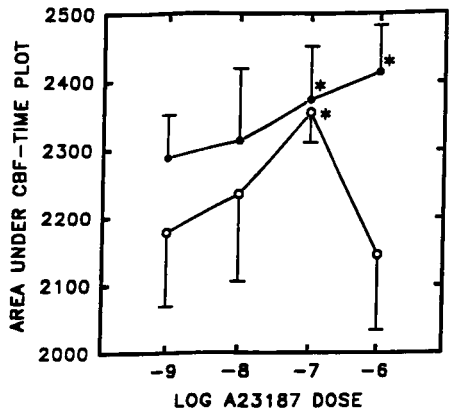

FIGURE 7 Dose-dependent stimulation of tracheal CBF by A23187, without (*closed circle*) and with (*open circle*) prior treatment of nifedipine, illustrated by the area under CBF-time plot versus log A23187 dose. * indicates $p < 0.001$ significance compared with baseline.

rechallenged with the ionophore. Significant attenuation was achieved only for the 10^{-8} M A23187 dose ($p < 0.001$) with a mean maximal stimulation of 10.0 Hz. The magnitude of tracheal CBF stimulatory responses induced by A23187 appeared to be temporally dependent (Fig. 8). The 2-min A23187 aerosolized challenge of the intact canine trachea produced significant ($p < 0.001$) delayed peak stimulation at 10^{-9} M (>20 min) and immediate peak (<2 min) stimulation at 10^{-8} ionophore doses.

DISCUSSION

Our previous observations indicating the episodic nature of the magnitude of CBF led to the development of stationary signal analysis to increase temporal resolution. We confirmed our previous observations regarding the magnitude of the stimulation induced by adrenergic and cholinergic autonomic agonists and again observed rapid temporal variations in the frequency at which cilia beat. The subsequent application of nonstationary signal analysis demonstrated a clearly defined 5.3-min periodicity of the cilia beat frequency which could be predictably synchronized between dogs in vivo by challenge with a calcium ionophore. The increase in CBF after this challenge was predominantly evident within a single period, thus potentially increasing the effective power of the cilia to transport mucus during this interval. The time for A23187 to induce this period-coupled tracheal CBF stimulation decreased with increasing doses of A23187. This is indicative of a one-compartment kinetic equation representing activation of the time-dependent magnitude component of the stimulation of tracheal CBF. This, together with a period-coupled component, is proposed as a CBF regulatory model consisting of a set of two coupled equations, each containing its own state variables; one controlling the magnitude and the other controlling the periodicity. The magnitude of the period-coupled stimulation of CBF was dependent on activation of voltage-operated calcium channels. The preservation of periodicity of CBF in the presence of nifedipine is consistent with our proposed CBF regulatory model. These are the first data to demonstrate that the magnitude and periodicity of CBF are two independent coupled processes. Thus, in addition to the one equation model describing amplitude modulation of ciliary wave behavior (Toremalm et al., 1975; Hybbinette and Mercke, 1982) mechanisms, there appears to exist an additional fundamental dynamic regulatory process whereby ciliary beat can respond to external perturbations.

FIGURE 8 Lapsed time for maximal tracheal CBF magnitude stimulatory responses after aerosolized A23187 challenge versus log A23187 dose.

The automation of the photon counting and spectral analysis procedures on a microcomputer ensures that CBF data were monitored and stored for future use in a rapid, uninterrupted, operator-independent, and objective manner. The real-time, on-screen display of tracheal CBF enabled continuous monitoring and the facilitation of experimentation (Eljamal et al., 1994; Yeates et al., 1992). This improved system had a frequency resolution of 1.3 Hz/channel, which is four times better than the hard-wired correlator using the same 3-ms sampling time. CBF measurements were missing due to the rejection of positive exponential autocorrelation functions in both the hard-wired correlator CALLS system and the automatic stationary PC-based system. When the hard-wired Langley-Ford correlator was used, any correlation that did not visually conform to an exponential decaying cosine function was discarded by the operator. The validity of this improved system incorporating both new hardware and software was evidenced by the consistent responses to the autonomic agonists between the stationary CBF system and the Langley-Ford correlator system.

Stationary correlation/Fourier transform allows the decomposition of the signal into individual frequencies. However, the power spectrum does not reveal the temporal relationships of the frequencies when they occur. The dominant frequency results from the beating of cilia within the envelope of the traveling metachronal wave. Thus, when the signal from the beating cilia is strong enough and/or the process is repeated several times, a dominant frequency is

evident using stationary signal analysis. As the oscillatory responses of CBF changed dynamically within seconds, as observed by us and others (Aiello et al., 1991; Ben-Shimol et al., 1991), further reduction of the photon collection time using the correlation/frequency stationary analysis did not generate reliable tracheal CBF measurements. This mix of frequencies was expected because the photons were backscattered from all the cilia that come in the purview of the 7-μm focal spot of the laser beam. Thus, a nonstationary time-frequency bilinear transformation was considered a more suitable alternative.

The ciliary beat pattern in vivo seems to exhibit an asymmetric beat with a modulated duty cycle. This is the first investigation to incorporate a kernel whose form, representing ciliary activity as represented by the scattered photons, has been proposed. The accuracy by which the CBF was measured using the nonstationary algorithm relied in part on the choice of the kernel. The exponential kernel of the Choi-Williams distribution, with its ability to suppress undesirable interactions due to cross-terms in multifrequency signals, appeared suited to identifying the dominant frequency from the motley of frequencies in the laser photon fluctuations. The design of the "cilia" kernel may require the generation of a data base of different ciliary beat patterns under different cellular physiological conditions. The adaptive processes introduced into the scaling factor, σ, of the kernel attempted to circumvent such problems. Due to the processing time of the 486 PC computer, more elaborate adaptive signal processing was not incorporated into the current algorithm. The selection of other kernels such as the Cone kernel (Jones and Parks, 1990, 1992; Loughlin et al., 1993) rather than the exponential kernel (the Choi-Williams distribution) may merit further consideration.

The use of a pentabarbitol-anesthetized canine model in which we have isolated the tracheal lumen and inhibited the neural and cyclooxygenase pathways, enabled the cellular mechanisms to be evaluated without the necessity of in vitro cell culture and its additional potential confounding factors. Thus, we can deduce from these studies that the periodic nature of CBF observed in this study is independent of neural input as well as cyclooxygenase products. Consistent with these data is the observation that ciliated cells exhibit spontaneous oscillations of CBF in vitro (Sanderson and Dirksen, 1990).

Using the nonstationary algorithm, the measurement of tracheal CBF in vivo in the intact canine model revealed similar temporal characteristics of the CBF magnitude responses to A23187. Whether this magnitude period-coupled stimulatory response was regulated by the calcium induced calcium release mechanism (Berridge et al., 1988; Berridge, 1993) or through the IP_3-Ca^{2+} cross-coupling mechanism (Meyer and Stryer, 1991) is uncertain. The delineation of this regulatory mechanism requires experimentation using specific agonists, such as α_1-agonist (Wong and Yeates, 1991) that can activate the receptor-operated mechanisms which could induce independent magnitude and periodicity stimulatory responses.

Oscillatory phenomena are an integral part of physiological systems, enabling them to respond easily and rapidly in both a temporal and spatial manner; ciliary beat, we have shown, is no exception. The magnitude and periodicity of CBF may control transport of mucus discretely through an amplitude controller or continuously through a period oscillator. When coupled cooperatively these mechanisms can be predicted to provide an efficient transport system. It is easy to conceive, however, that when such processes are decoupled, nonlinear relationships between CBF and mucociliary transport can be anticipated. Such decoupling could lead to erratic and abnormal mucus transport.

The discovery of the oscillatory nature of CBF in vivo requires that these observations be incorporated into an integral picture of how the mucociliary transport system may operate. Mucus has been shown to be transported up the trachea in a linear manner consistent with mucus streaming as previously described (Hilding, 1957). When radiotagged aerosols deposited on airway bifurcations are observed by γ scintigraphy they appear to "move off" their deposition site in an intermittent manner leading to a relatively large variability in large-airway transit time (Yeates, 1988). However, once a bolus starts moving it continues to be transported up the trachea (personal observation). It has been observed in rats that mucus appears to be transported as discrete plaques (Van As, 1972). Taking these observations in concert with our findings on the periodic nature of ciliary beat leads us to propose the following descriptive model of mucociliary clearance. Cilia beat in a periodic manner in which the periodicity is of a low amplitude. When stimulated, an increase in the magnitude of CBF superimposed on the periodicity is anticipated to cause any mucus atop the cilia to be transported. This implies that this localized activation of ciliary activity travels up the airway at the same rate as mucus is transported up the airway and that the increase in beat frequency transmitted by the cell to the cilia precedes the mucus "plaque" or "raft" being transported. Such coordination is required to avoid local accumulation of mucus at the leading edge and to maintain the "sheet"-like protective nature of the mucus coating. A phenomenon which could explain such a mechanism is the observation that calcium "waves" were propagated at approximately 2 mm/min in tracheal epithelial cells (Sanderson et al., 1990). These concepts are consistent with and expand our previous model in which the cilia beat in the direction of the longitudinal axis of the airway within the envelope of an antipletic metachronal wave that has an angle of declination with respect to this axis (Wong et al., 1993). Thus the ciliary "escalator" does not seem to behave like a mechanical escalator or conveyor belt that is constantly on, but rather contains control mechanisms that regulate its operation when necessary but also allows for quiescent periods, a feature fundamental to most organ systems and organelles. This provides an alternate regulatory mechanism whereby mucus can feed sequentially into larger airways avoiding a local accumulation of mucus. Such a system would avoid the severe constraints of predicted "water and mucus" absorption proposed in a model (Kilburn, 1968) that

contained a mucus layer of uniform depth in the airways whose circumference converges some 100,000 times. This notion is consistent with the concept that mucus transport in the very small airways is not a few microns per minute as indicated by mathematical models (Yeates and Aspin, 1978; Yeates et al., 1981) but rather these predicted mucus transport rates represent an "average" transport velocity with mucus being transported episodically at realistic rates. Such periodic systems integrated throughout the converging airways may provide a reserve such that hypersecretion produced by irritants can be successfully transported and removed without airway plugging. The above-mentioned decoupling of the CBF regulatory mechanisms could lead to the erratic clearance of secretions and pathologic sequelae as observed in patients with chronic obstructive pulmonary disease (Yeates, 1982).

This work is based on a thesis of T. Chandra, submitted in partial fulfillment of the requirements for the Ph.D. degree in Chemical Engineering at the University of Illinois at Chicago. The authors would like to thank Dr. Brian Duff for performing the electroporated surgical procedure. Fenoterol was supplied by Boehringer Ingelheim. This work was presented in part at the 1991 American Physiological Society Meeting.

This work was supported by the National Institutes of Health (ES04317, HL46376), the Whitaker Foundation, and the Veterans Administration, West Side.

REFERENCES

Aiello, E., J. Kennedy, and C. Hernandez. 1991. Stimulation of frog ciliated cells in culture by acetylcholine and substance P. *Comp. Biochem. Physiol.* 99C:497–506.

Ben-Shimol, Y. Its'Hak Dinstein, A. Meisels, and Z. Priel. 1991. Ciliary motion features from digitized video photography. *J. Comput. Assisted Microsc.* 3:103–116.

Berridge, M.J. 1993. Inositol triphosphate and calcium signalling. *Nature.* 361:315–325.

Berridge, M.J., P.H. Cobbold, and K.S.R. Cuthbertson. 1988. Spatial and temporal aspects of cell signalling. *Philos. Trans. R. Soc. Lond. B. Biol. Sci.* 320:325–343.

Chandra, T. 1992. Regulation of nonstationary cellular dynamics and chaotic respiratory rhythm in vivo. Ph.D. thesis. University of Illinois at Chicago.

Choi, H.I., and W.J. Williams. 1989. Improved time-frequency representation of multicomponent signals using exponential kernels. *IEEE (Inst. Electr. Electron. Eng.) Trans. Acoust. Speech Signal Process.* 37:862–871.

Cohen, L. 1966. Generalized phase-space distribution function. *J. Math. Phys.* 7:781–786.

Cohen, L. 1989. Time-frequency distributions—A review. *Proc. IEEE.* 77: 941–981.

Cummins, H.Z., and H.L. Swinney. 1970. Light beating spectroscopy. *In* Progress in Optics. E. Wolf, editor. Vol. 8. Academic Press. 135–200.

Di Benedetto, G., C.J. Magnus, P.T.A. Gray, and A. Mehta. 1991. Calcium regulation of ciliary beat frequency in human respiratory epithelium in vitro. *J. Physiol. (Lond.).* 439:103–113.

Dirksen, E.R., and M.J. Sanderson. 1990. Regulation of ciliary activity in the mammalian respiratory tract. *Biorheology.* 27:533–545.

Duff, B.E., B.L. Wenig, E. Applebaum, L.D. Hollinger, and D.B. Yeates. 1992. Tracheal reconstruction using an epithelial equivalent. American Laryngological, Rhinological and Otological Society, Inc. (The Tiological Society).

Eljamal, M., L.B. Wong, and D.B. Yeates. 1994. Capsaicin activated bronchial and alveolar initiated pathways regulating tracheal ciliary beat frequency. *J. Appl. Physiol.* In press.

Finsy, R., P. de Groen, L. Deriemaeker, and M. van Laethem. 1989. Singular value analysis and reconstruction of photon correlation data equidistant in time. *J. Chem. Phys.* 91:7374–7383.

Girard, P.R., and J.R. Kennedy. 1989. Calcium regulation of ciliary activity in rabbit tracheal epithelial explants and outgrowths. *Eur. J. Cell Biol.* 40:203–209.

Golub, G.H., and C.F. Van Loan. 1983. Matrix computations. John's Hopkins University Press, Baltimore. Chapter 2.3.

Hameister, W.M., L.B. Wong, and D.B. Yeates. 1991. Tracheal ciliary beat frequency in baboons: effects of peripheral histamine and capsaicin. *Agents Actions.* 35:200–207.

Harrison, R.A., L.B. Wong, and D.B. Yeates. 1992. Short-term interaction of airway and tissue oxygen tensions on ciliary beat frequency in dogs. *Am. Rev. Respir. Dis.* 146:141–147.

Haykin, S. 1991. Adaptive Filter Theory. 2nd ed. Prentice Hall, Englewood Cliffs, NJ. 854 pp.

Hilding, A.C. 1957. Ciliary streaming in lower respiratory tract. *Am. J. Physiol.* 191:404–410.

Hlawatsch, F., and G.F. Boudreaux-Bartels. 1992. Linear and quadratic time-frequency signal representations. *IEEE SP Magazine.* 9:21–67.

Hybbinette, J.C., and U. Mercke. 1982. A method for evaluating the effect of pharmacological substances on mucociliary activity in vivo. *Acta Otolaryngol.* 93:151–159.

Jakeman, E. 1974. Photon correlation. *In* Photon-correlation and Light-beating Spectroscopy. J. Jakeman, H.Z. Cummins, E.R. Pike, editors. NATO Press, New York. 75–149.

Jones, D.L., and T.W. Parks. 1990. A high resolution data-adaptive time frequency representation. *IEEE (Inst. Electr. Electron. Eng.) Trans. Acoust. Speech Signal Process.* 38:2127–2135.

Jones, D.L., and T.W. Parks. 1992. A resolution comparison of several time-frequency representation. *IEEE (Inst. Electr. Electron. Eng.) Trans. Acoust. Speech Signal Process.* 40:413–420.

Kilburn, K.H. 1968. A hypothesis for pulmonary clearance and its implications. *Am. Rev. Respir. Dis.* 98:449–463.

Lee, W.I., and P. Verdugo. 1976. Laser light scattering spectroscopy: a new application in the study of ciliary activity. *Biophys. J.* 16:1115–1119.

Loudon, R. 1983. The Quantum Theory of Light. 2nd ed. Clarendon Press, Oxford. 393 pp.

Loughlin, P.J., J.W. Pitton, and L.E. Atlas. 1993. Bilinear time-frequency representations: new insights and properties. *IEEE (Inst. Electr. Electron. Eng.) Trans. Acoust. Speech Signal Process.* 41:750–767.

Meyer, T., and L. Stryer. 1991. Calcium spiking. *Annu. Rev. Biophys. Biophys. Chem.* 20:153–174.

Oliver, C.J. 1974. Correlation techniques. *In* Photon Correlation and Light Beating Spectroscopy. H.Z. Cummins and E.R. Pike, editors. Plenum, New York. 151–223.

Oliver, C.J. 1979. Spectral analysis with short data batches. *J. Phys. A. Math. Gen.* 2:591–617.

Oliver, C.J. 1980. Recent developments in photon correlation and spectrum analysis techniques: II. Information from photodetection spectroscopy. In Scattering Techniques Applied to Supramolecular and Nonequilibrium Systems. S.H. Chen, B. Chu and R. Nossal editors. Plenum Press, New York. 121–160.

Oppenheim, A.V., and R.W. Schafer. 1975. Digital Signal Processing. *Prentice Hall, Englewood Cliffs, NJ. 585 pp.*

Pressman, B.C. 1976. Biological applications of ionophores. Annu. Rev. Biochem. 45:501–530.

Rapp, P.E. 1987. Why are so many biological systems periodic? *Prog. Neurobiol.* 29:261–273.

Sanderson, M.J., A.C. Charles, and E.R. Dirksen. 1990. Mechanical stimulation and intercellular communication increases intracellular Ca^{+2} in epithelial cells. *Cell Regul.* 1:585–596.

Sanderson, M.J., and E.R. Dirksen. 1990. Mechanosensitive and beta-adrenergic control of the ciliary beat frequency of mammalian respiratory tract cells in culture. *Am. Rev. Resp. Dis.* 139:432–440.

Toremalm, N.G., C.H. Hakansson, U. Mercke, and B. Dahlerus. 1975. Mucociliary wave pattern: an analysis of surface light reflections. *Acta Otolarygol. (Stockh).* 78:247–252.

Van As, A. 1972. The organization of ciliary activity and mucus transport in pulmonary airways. *S. Afr. Med. J.* 46:347–350.

Villalon M., T.R. Hinds, and P. Verdugo. 1989. Stimulus-response coupling in mammalian ciliated cells: Demonstration of two mechanisms of control for cytosolic [Ca^{2+}]. *Biophys. J.* 56:1255–1258.

Wijnaendts van Resandts, R.W. 1974. A digital autocorrelator for quasi-elastic light scattering using a minicomputer. *Rev. Sci. Instrum.* 45:1507–1510.

Wong, L.B., I.F. Miller, and D.B. Yeates. 1988a. Stimulation of ciliary beat frequency by autonomic agonists: *in vivo*. *J. Appl. Physiol.* 65:971–981.

Wong, L.B., Miller, I.F., and Yeates, D.B. 1988b. Stimulation of ciliary beat frequency by autonomic agonists *in vitro*. *J. Appl. Physiol.* 65:1967–1971.

Wong, L.B., I.F. Miller, and D.B. Yeates. 1990a. Regulatory pathways for the stimulation of canine tracheal ciliary beat frequency by bradykinin. *J. Physiol. (Lond.).* 422:421–431.

Wong, L.B., I.F. Miller, and D.B. Yeates. 1990b. Stimulation of tracheal ciliary beat frequency by capsaicin. *J. Appl. Physiol.* 68:2574–2580.

Wong, L.B., I.F. Miller, and D.B. Yeates. 1991. Pathways of substance P stimulation of canine tracheal ciliary beat frequency. *J. Appl. Physiol.* 70:267–273.

Wong, L.B., I.F. Miller, and D.B. Yeates. 1993. Nature of the mammalian ciliary metachronal wave. *J. Appl. Physiol.* 75:458–467.

Wong, L.B., and D.B. Yeates. 1991. Alpha 1 receptor activation stimulates ciliary beat frequency through an IP3 induced influx of extracellular calcium. *Am. Rev. Respir. Dis.* 143(2 P2):A138.

Yeates, D.B. 1982. The role of mucociliary transport in the pathogenesis of chronic obstructive pulmonary disease. *In* Mucus in Health and Disease II. E.N. Chantler, J.B. Elder, and M. Elstein, editors. Plenum Press, New York. 411–415.

Yeates, D.B. 1988. Radioaerosol technique. *In* Methods in Bronchial Mucology. P.C. Braga and L. Allerga, editors. Raven Press, New York. 357–365.

Yeates, D.B., and N. Aspin. 1978. A mathematical description of the airways of the human lungs. *Respir. Physiol.* 32:91–104.

Yeates, D.B., Eljamal, M., Wong, L.B., and Miller, I.F. 1992. Cellular-neural-cellular pathways mediating the response of tracheal ciliary beat frequency (CBF_t) to inhaled capsaicin. *Chest.* 101(Suppl.):72s–73s.

Yeates, D.B., T.R. Gerrity, and C.S. Garrard. 1981. Particle desposition and clearance in the bronchial tree. *Ann. Biomed. Eng.* 9:577–592.

Zeiger, H.P., and A.J. McEwen. 1974. Approximate realization of given dimension via Ho's algorithm. *IEEE Trans. Automat. Control.* AC-19: 153.